Interlaminar Fracture Characteristics of Tougher Thermoset Materials

R. C. Shah,* G. Miliziano,* and A. V. Viswanathan†
Boeing Military Airplane Company, Seattle, Washington

Critical strain energy release rates G_{Ic} for interlaminar fracture were determined under pure mode I loading conditions for tougher thermoset material systems AS6/2220-3 and AS6/5245C. G_{Ic} values were determined with constant-width, double-cantilever beam specimens for room temperature (RT)/dry, RT/wet, and −75°F/dry conditions. The critical strain energy release rates G_{Tc} under mixed mode I-II loading conditions were also determined for these materials with cracked lap shear (CLS) specimens for RT/dry and RT/wet conditions. Both AS6/2220-3 and AS6/5245C material systems have significantly higher interlaminar fracture toughness compared to currently used composite systems such as T300/5208. Delamination growth rates da/dN were also determined experimentally for the above material systems under pure mode I and mixed mode I-II loading conditions for the above-mentioned environmental conditions. Delamination growth rates were plotted and correlated with the maximum applied strain energy release rate G_I or G_T. Growth rate equations were determined for each material and environmental condition. Delamination growth rates were also compared with those of the T300/5208 system. da/dN for AS6/5245C for RT/wet environment is significantly higher than that for RT/dry conditions. Striation markings were observed for CLS specimens. Delamination growth rates vs G_{Tmax} from striations correlated very well with those from visually observed crack length data.

Nomenclature

a	= delamination or crack length
b	= specimen width
C	= compliance of specimen
C_1, n	= delamination growth rate equation constant and exponent
CLS	= crack lap shear
DCB	= double-cantilever beam
G	= strain energy release rate
N	= number of loading cycles
P	= applied load
R	= minimum to maximum cyclic stress or load ratio
RT	= room temperature
δ	= cross-head deflection or opening displacement

Subscripts

I,II	= mode I or mode II
T	= total mixed mode
c,cr	= critical
max	= at maximum stress during a loading cycle
min	= at minimum stress during a loading cycle
TH	= threshold

I. Background

DELAMINATIONS most commonly originate due to voids occurring during laminate processing and/or damage caused during assembly or subsequent service and loading conditions and/or to local stress raisers. The presence and growth of delaminations can significantly affect the residual strength as well as life of the composite structure. Considerable work has been recently performed to define delamination behavior under static and cyclic loading conditions for currently used graphite-epoxy systems.[1-10] Resistance to impact damage and delamination can be improved with materials having tougher resins. Tougher materials enable the use of higher allowable design strains and enhance structural efficiency.

A double-cantilever beam (DCB) specimen has been used by several investigators[3-9] to determine mode I delamination or interlaminar fracture characteristics of graphite/epoxy materials. A cracked lap shear (CLS) specimen has been used to determine mixed mode I-II fracture characteristics of these materials.[3-5]

The objective of the work reported in this paper was to determine critical strain energy release rates and delamination growth rates under constant amplitude cyclic loading for mode I and mixed modes I-II loading conditions for tougher thermoset materials AS6/2220-3 and AS6/5245C. An experimental program was conducted to determine the above values for room temperature (RT)/dry, RT/wet, and −75°F/dry conditions. The fracture surfaces of CLS specimens were examined with scanning and traveling electron microscopes (SEM and TEM) and revealed striation markings.

II. Materials and Experimental Procedures

Materials

Advanced material systems with higher fracture toughness AS6/2220-3 and AS6/5245C graphite-epoxy systems were selected for testing. Grade 190 graphite-epoxy prepreg tape was used to make laminates for the test specimens. Various property measurements for a six-ply, 0° laminate are shown in Table 1.

Test Program and Specimens

Tests were conducted on 14 specimens of AS6/2220-3 and 18 specimens of AS6/5245C material systems to evaluate mode I interlaminar critical strain energy release rates and

Presented as Paper 85-0609 at the AIAA/ASME/ASCE/AHS 26th Structures, Structural Dynamics and Materials Conference, Orlando, FL, April 15-17, 1985; received May 13, 1985; revision submitted March 13, 1986. Copyright © American Institute of Aeronautics and Astronautics, Inc., 1986. All rights reserved.

*Principal Engineer, Senior Specialist Engineer.
†Supervisor. Associate Fellow AIAA.

delamination growth rates for RT/dry, RT/wet, and −75°F/dry environmental conditions. Test conditions and number of tests per condition are shown in Table 2. A schematic of constant width DCB test specimen is shown in Fig. 1. Each specimen consisted of 24 plies of 0° material, with a folded 1 mil thick Kapton film 1 in. long at the loading end between plies 12 and 13.

Test Procedures

All DCB and CLS specimen tests were conducted in a displacement-controlled mode to obtain stable delamination growth under applied loading. Constant-amplitude fatigue tests were conducted at a frequency of 5 Hz and minimum to maximum load (or displacement) ratio $R = 0.05$. All DCB tests were conducted in a 20,000 lb capacity MTS test machine equipped with a Baldwin-Lima-Hamilton (BLH) 50 lb load cell. The test machine actuator displacement was controlled and the resultant load was monitored and recorded. Crack lengths were visually measured and recorded with a low-power magnifier. Actuator displacement and specimen crack opening for DCB specimens were assumed to be the same.

Loads were introduced through the flexible aluminum tabs, ensuring a pure mode I delamination growth over the specimen length. For each material type, all specimens were cut from a single 12.0 × 30.0 in. panel to ensure consistency in material properties. Specimen edges were painted with white enamel paint and indelible ink lines were drawn at 0.10 in. intervals to aid measurement of crack lengths.

Sixteen CLS specimens were tested to evaluate combined mode I-II interlaminar critical strain energy release rates and delamination growth rates. The test matrix for these tests is shown in Table 2. As shown in Table 2, eight specimens were fabricated for each material system. The laminates for CLS specimens have 16 plies with a layup stacking sequence of $(0_2/\pm 45/\mp 45/0_2)_s$ in the region of the maximum thickness, as shown in Fig. 2. A 1 mil thick Kapton film is folded between the two 0° plies at the laminate midplane with 1.0 in. long initial delamination at the step location. Details of the fabricated specimen configuration are shown in Fig. 2. For each material type, all specimens were machined from a single 40.0 × 38.0 in. panel and specimen edges were painted and marked as described for DCB tests.

For static DCB tests, the rate of actuator displacement was manually adjusted. The cross-head speed was 0.05 in./s. Displacement was increased until an initial sharp delamination beyond the implanted Kapton was formed. The deflection, the loads at crack initiation and arrest, and the arrested crack

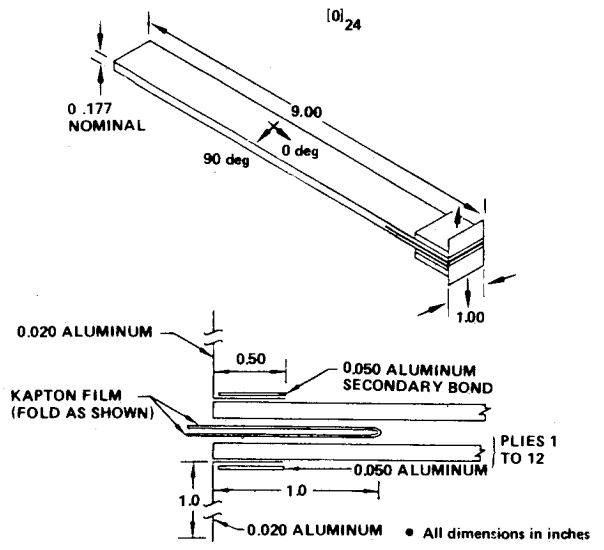

Fig. 1 Mode I DCB specimen.

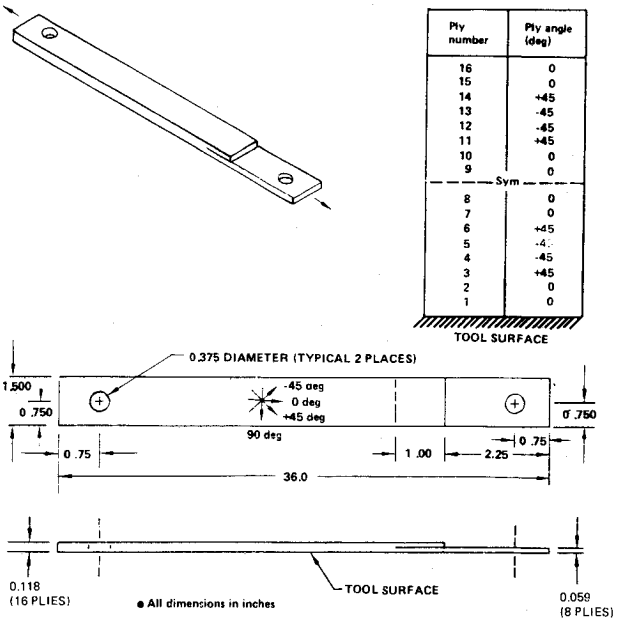

Fig. 2 Mixed-mode CLS specimen.

Table 1 Material property measurements

Material	Resin content, wgt %	Areal fiber weight, g/m²	Property measurement 0°tension laminate: Failure stress, ksi	Failure strain, μin./in.	Modulus, Msi	180°F failure stress for 0° compression laminate: Dry, ksi	Wet (24 day soak), ksi
AS6/2220-3	34.2	193	320	16,100	19.9	160	160
AS6/5245C	32.5	189	286	15,500	18.4	176	179

Table 2 Test matrix for modes I and I-II static and cyclic tests

Material	Specimen type	No. of static tests: RT/dry	RT/wet	−75°F/dry	No. of cyclic tests: RT/dry	RT/wet	−75°F/dry
AS6/2220-3	DCB	3	2	2	3	2	2
	CLS	3	—	—	3	2	—
AS6/5245C	DCB	6	2	2	4	2	2
	CLS	3	—	—	3	2	—

length were recorded. The deflection was decreased until a zero load was observed. The deflection was then increased until several crack initiations and arrests were observed and then decreased until a zero load was observed. The process was repeated several times until the crack length was greater than 2.0 in.

Prior to the constant-amplitude fatigue cycling of the DCB specimens, the specimen/actuator deflection was increased until an initial sharp delamination was formed as discussed above. The deflection was then decreased until the load registered zero, then increased until the autographic record of the load vs deflection curve indicated a maximum load had been reached. The deflection at this maximum load was the maximum cyclic deflection parameter. The minimum deflection parameter was established at a stress ratio of $R=0.05$. The rate of cycling was 5 Hz. The crack length, number of applied deflection cycles, and load were recorded for a unique maximum deflection. Each fatigue specimen was subjected to cycling at more than one deflection, with data generated for each unique deflection.

Test procedures for the static and cyclic CLS tests were similar to those for the DCB specimens. The CLS specimens were tested in a 50 kip capacity MTS test machine. The applied displacement on CLS specimens was assumed to be the same as the relative displacement between the grips.

Prior to the fatigue or static testing of the DCB or CLS specimens, the specimens for RT/wet tests were conditioned in an environmental chamber at a temperature of 170°F and a relative humidity of 85%. The mode I DCB specimens were left in the chamber for 150 days. Moisture saturation was attained and the moisture contents by weight for AS6/2220-3 and AS6/5245C specimens were 1.05 and 0.95%, respectively.

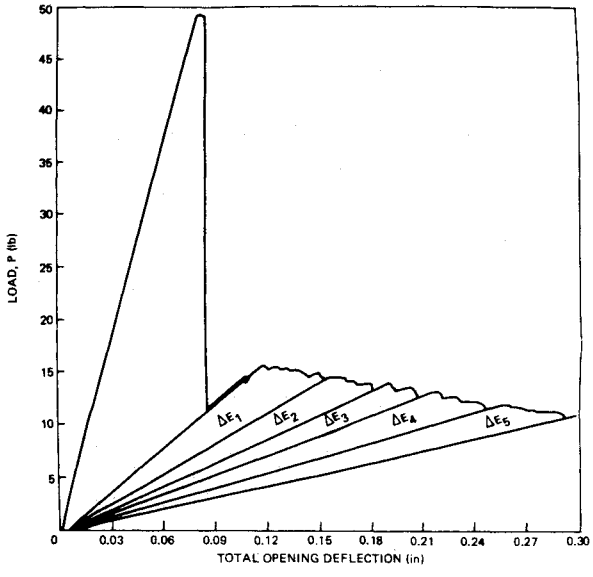

Fig. 3 Typical load-deflection plot for mode I static DCB test.

Table 3 G_{Ic} values for AS6/2220-3

Specimen number	Conditions	G_{Ic} values, lb-in./in.^{2}	Average G_{Ic} values, lb-in./in.^{2}
7208-2	RT/dry	1.31	
7208-4	RT/dry	1.16	1.21
7208-11	RT/dry	1.17	
7209-9	RT/wet	1.35	1.34
7208-10	RT/wet	1.33	
7208-15	−75°F/dry	1.06	1.08
7208-16	−75°F/dry	1.10	

The mode II CLS specimens were exposed in the chamber for 110 days. Moisture saturation was attained only for the AS6/2220-3 specimens. The moisture contents by weight for AS6/2220-3 and AS6/5245C specimens were 0.93 and 0.87%, respectively. The wet specimens were individually removed from the chamber and wrapped in damp towels and plastic to retain their moisture. The specimens tested at −75°F were encased in a Styrofoam box. Gaseous liquid nitrogen was introduced into the box via a cryogenic solenoid valve modulated by a Wahl temperature controller using type K thermocouples attached to the specimen. Delamination length measurements were visually obtained through double-paned acrylic panels built into the box.

III. Test Results and Discussion

Static Fracture Tests

AS6/2220-3 and AS6/5245C DCB specimens were tested to determine the critical strain energy release rates G_{Ic} in RT/dry, RT/wet, and −75°F/dry environmental conditions. Figure 3 shows a typical load vs total opening deflection plot for a mode I DCB specimen. Individual values of the critical strain energy release rates G_{Ic} were computed using the following equation based on the area method,[9] which evaluates the strain energy release ΔE_i due to the crack extension Δa_i:

$$G_{Ic}=\Delta E_i/b\Delta a_i \tag{1}$$

An average value of G_{Ic} was determined[9] using a series of N crack extensions of Δa_i and corresponding ΔE_i as

$$G_{Ic}=\frac{1}{bN}\sum_{i=1}^{N}\frac{\Delta E_i}{\Delta a_i} \tag{2}$$

where ΔE_i is the change in area of the load deflection curve in pound-inches and Δa_i the change in crack length corresponding ΔE_i in inches

This is the same as the area under the load displacement curve after the initiation of delamination divided by the product of the total crack extension, Δa and b.

Individual as well as average G_{Ic} values were calculated using Eqs. (1) and (2) for each specimen. Average values of G_{Ic} for each specimen are shown in Tables 3 and 4 for AS6/2220-3 and AS6/5245C materials, respectively. In the case of

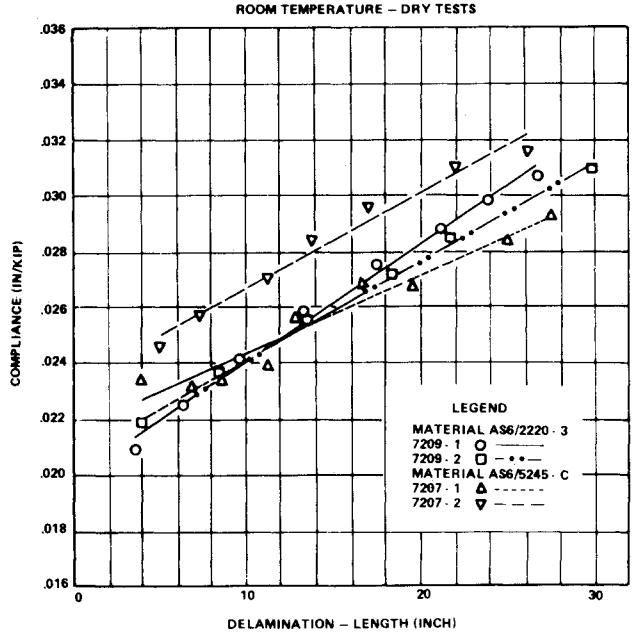

Fig. 4 Typical compliance vs delamination length plots for static CLS tests.

AS6/2220-3 tests, the individual values of G_{Ic} were, in general, in good agreement with the average G_{Ic} for the specimen. For AS6/5245C tests, as shown in Table 5 for a typical case, individual values of G_{Ic} increased as the crack length increased. In Table 5, a_i and a_f pertain to the delamination length at the initiation and the arrest (or unloading) time, respectively. Fiber bridging was observed in some specimens of AS6/5245C only. G_{Ic} vaues for specimens with the fiber bridging are higher and were not included in computing the average G_{Ic} value in Table 4. G_{Ic} values for AS6/2220-3 material at RT/dry, RT/wet, and $-75°$F/dry, as shown in Table 3, are 1.21, 1.34, and 1.08 lb-in./in.^{2}, respectively. G_{Ic} values for AS6/5245C material at RT/dry, RT/wet, and $-75°$F/dry are 2.05, 1.88, and 1.97 lb-in./in.^{2}, respectively.

Results for AS6/2220-3 show that RT/wet and $-75°$F/dry G_{Ic} is within $\pm 10\%$ of the RT/dry G_{Ic} value. Considering normal scatter, it can be said that G_{Ic} for AS6/2220-3 is nearly unaffected by RT/dry, RT/wet, or $-75°$F/dry environments. G_{Ic} for AS6/5245C in RT/wet and $-75°$F/dry is 8 and 4% lower than that in RT/dry environment, respectively. Both the AS6/2220-3 and AS6/5245C material systems are significantly tougher than the T300/5208 system for which $G_{Ic} \simeq 0.5$ lb-in./in.^{2}.

Tests were conducted on AS6/2220-3 and AS6/5245C CLS specimens to determine mixed mode I-II critical strain energy release rates G_{Tc} in RT/dry and RT/wet environments. A mixed mode CLS specimen of Fig. 2 typically induced $G_I \simeq 0.20\ G_T$ and $G_{II} \simeq 0.80\ G_T$, where G_I, G_{II}, and G_T are mode I, mode II, and the total mixed mode strain energy release rates, respectively.[4,5] Initially, tests were conducted on 36.0 in. long specimens with the intent of obtaining many sets of delamination growth and arrest and G_{Tc} values from one CLS specimen loaded in a displacement controlled mode. An average value of G_{Tc} was computed using the area method of a series of N crack extensions of Δa_i and using Eq. (2) where G_{Ic} is replaced by G_{Tc}. The total critical strain energy release rate was also calculated for each delamination growth and arrest value from the compliance method by

$$G_{Tc} = \frac{P_{cr}^2}{2b} \frac{dC}{da} \tag{3}$$

where P_{cr} is the critical load at which delamination arrests.

Figure 4 shows the typical compliance vs delamination length plots for static CLS specimen tests conducted in a RT/dry environment for both materials. The actual test data as well as the fitted least-square straight lines are shown in the figure. These compliance vs delamination plots, as well as all other similar plots for static and cyclic tests, showed that the compliance C is well represented by a linear equation of a, as

$$C = Aa + B \tag{4}$$

where A and B are constants. dC/da; hence, G_T or G_{Tc} is independent of the delamination length a.

Table 4 G_{Ic} values for AS6/5245-C

Specimen number	Conditions	G_{Ic} values, lb-in./in.^{2}	Average G_{Ic} values, lb-in./in.^{2}
7206-5	RT/dry	1.89	
7206-6	RT/dry	1.83	
7206-7[a]	RT/dry	2.37[a]	2.05
7206-8[a]	RT/dry	3.18[a]	
7206-14	RT/dry	1.91	
7206-17	RT/dry	2.56	
7206-9	RT/wet	2.10	1.88
7206-10	RT/wet	1.65	
7206-15	$-75°$F/dry	1.83	1.97
7208-16	$-75°$F/dry	2.10	

[a]Fiber bridging, not included in average G_{Ic} computation.

For each delamination growth and arrest condition, individual G_{Tc} value was computed from area and compliance methods [Eqs. (1) and (3)]. The average of those individual G_{Tc} values for each specimen is shown in Tables 6 and 7 for AS6/2220-3 and AS6/5245C, respectively. A significant variation in individual G_{Tc} values was observed for some specimens. For example, the high value of G_{Tc} was 2.0 and 1.5 times as large as the low value of G_{Tc} for the compliance and the area method, respectively, for some static test specimens. As seen from Tables 6 and 7, G_{Tc} values for some specimens were obtained from specimens used in cyclic tests. G_{Tc} computed from the area method was slightly higher (less than 8% except for RT/wet tests of AS6/5245C) than the G_{Tc} from the compliance method. Thus, the area method G_{Tc} is used in the ensuing discussion. G_{Tc} values at RT/dry and RT/wet are 2.93 and 2.33 lb-in./in.^{2} for AS6/2220-3 and 3.07 and 2.38 lb-in./in.^{2} for AS6/5245C. These results show that G_{Tc} for the RT/wet environment is approximately 80% of G_{Tc} for the RT/dry environment. Comparing G_{Tc} for RT/dry conditions with the corresponding G_{Ic} values, it is found that $G_{Tc} \simeq 2.4\ G_{Ic}$ for AS6/2220-3 and $\simeq 1.5\ G_{Ic}$ for AS6/5245C. G_{Tc} for the RT/dry condition for T300/5208 material[4] is 2.3 lb-in./in.^{2} G_{Tc} for AS6/2220-3 and AS6/5245C is approximately 30% higher than G_{Tc} for T300/5208 at RT/dry conditions. Compared to G_{Tc} of these three materials, G_{Ic} values of these materials have wide differences.

Six 10.0 in. long and 0.5 in. wide (all 0°) 8 and 10 ply thick CLS specimens of AS6/5245C and AS6/2220-3 were also tested in RT/dry conditions. G_{Tc} values obtained from these tests are 2.65 and 3.28 lb-in./in.^{2} for AS6/2220-3 and AS6/5245C, respectively. These G_{Tc} values are within 10% of the corresponding G_{Tc} values for 36.0 in. long CLS specimens.

As mentioned before, G_{II} forms the major portion of G_{Tc} ($G_{II} \simeq 0.8\ G_{Tc}$). Also for all these material tested, G_{Ic} is less than G_{Tc}. From these results, it is safe to assume that pure mode II critical strain energy release rate G_{IIc} must be greater than G_{Tc}.

Cyclic Tests

Constant-amplitude fatigue tests on mode I DCB specimens were conducted to determine the delamination growth rate relationships with the applied strain energy release rates. A typical plot of measured crack length a vs the number of applied cycles N and applied load P vs the number of applied cycles for the mode I fatigue test is shown in Fig. 5. These measured values of a and P are smoothed out with a least-square curve fitting. Since the specimen is cycled under the applied constant maximum (and minimum) displacement load as well as a computed strain energy release rate, G_I reduces as the crack length increases. The strain energy release rate G_I for a constant-amplitude mode I cyclic loading was computed using the beam analysis equation,[8,9]

$$G_I = 3P\delta/2ba \tag{5}$$

Table 5 Individual G_{Ic} values for AS6/5245C for RT/dry condition (specimen no. 7206-17)[a]

ΔE, lb-in./in.	a_f, in.	a_i, in.	Δa, in.	G_{Ic}, lb-in./in.^{2}
0.378	1.32	1.10	0.22	1.720
0.738	1.70	1.32	0.38	1.942
0.603	2.00	1.70	0.30	2.010
1.578	2.63	2.00	0.63	2.505
1.690	3.23	2.63	0.60	2.817
1.507	3.76	3.23	0.53	2.843
1.918	4.40	3.76	0.64	3.000
1.235	4.80	4.40	0.40	3.088
0.859	5.08	4.80	0.28	3.068

[a]Average $G_{Ic} = 2.56$ lb-in./in.^{2}

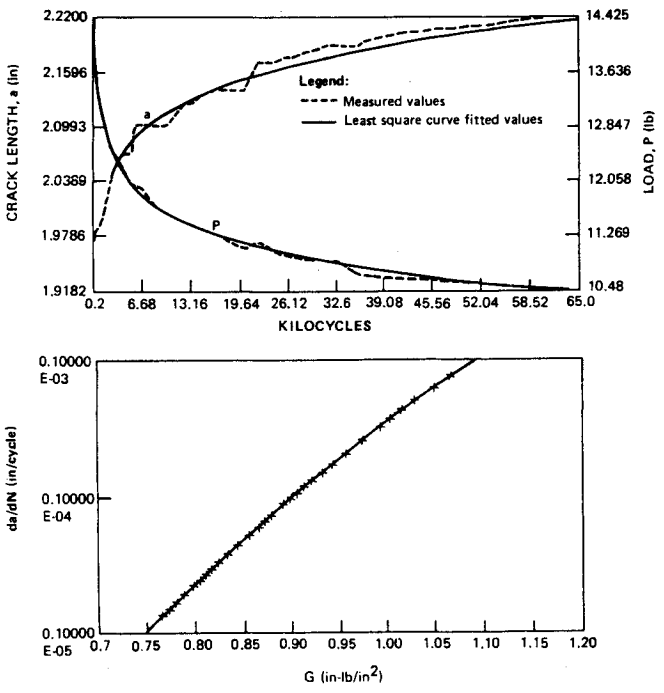

Fig. 5 Typical mode I fatigue test data and data reduction.

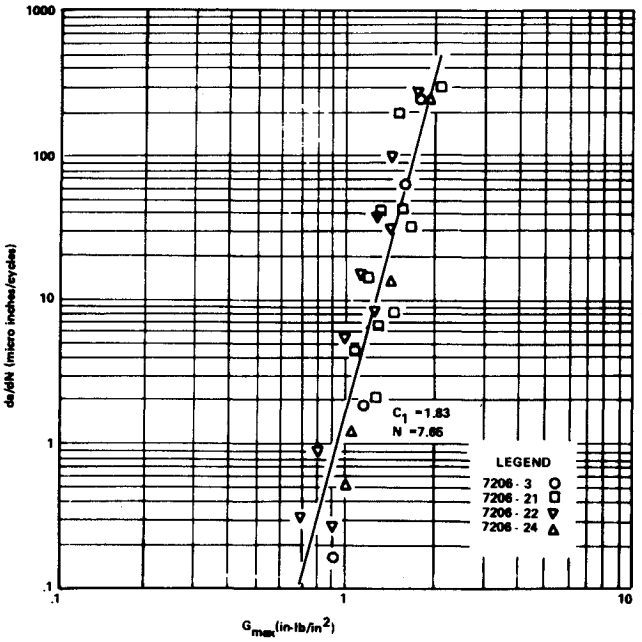

Fig. 6 Delamination growth rates for AS6/5245C in RT/dry environment.

Table 6 G_{Tc} values for AS6/2220-3

Specimen no.	Conditions	G_{Tc}, lb-in./in.^{2} From area method	G_{Tc}, lb-in./in.^{2} From compliance method	Average G_{Tc}, lb-in./in.^{2} From area method	Average G_{Tc}, lb-in./in.^{2} From compliance method
7209-1	RT/dry	2.84	2.87		
7209-2	RT/dry	2.78	2.77		
7209-5[a]	RT/dry	3.17	2.74	2.93	2.72
7209-6[a]	RT/dry	—	2.98		
7209-11[a]	RT/dry	—	2.26		
7209-7[a]	RT/wet	2.69	2.77	2.33	2.20
7209-10[a]	RT/wet	1.98	1.63		

[a]Cyclic test specimen.

Table 7 G_{Tc} values for AS6/5245C

Specimen no.	Conditions	G_{Tc}, lb-in./in.^{2} From area method	G_{Tc}, lb-in./in.^{2} From compliance method	Average G_{Tc}, lb-in./in.^{2} From area method	Average G_{Tc}, lb-in./in.^{2} From compliance method
7207-1	RT/dry	2.50	2.34		
7207-2	RT/dry	3.20	2.57		
7207-3	RT/dry	3.50	3.40	3.07	2.89
7207-5[a]	RT/dry	—	3.22		
7207-6[a]	RT/dry	—	2.93		
7207-9[a]	RT/wet	2.37	2.03	2.38	2.00
7207-10[a]	RT/wet	2.40	1.97		

[a]Cyclic test specimen.

where P is the measured load at delamination length a and δ the cross-head deflection corresponding to P.

The computed plot of da/dN vs G_I is also shown in Fig. 5. A typical data plot of da/dN vs G_{max} is shown in Fig. 6. A general delamination growth rate equation encompassing all three regions of growth (region I of growth near the threshold, region II growth in the stable region, and region III of rapid growth near the critical G region) can be expressed by

$$\frac{da}{dN} = \frac{CG_{max}^{m}(\Delta G - \Delta G_{TH})^{n}}{(G_c - G_{max})^{P}} \quad (6)$$

where:

ΔG = $G_{max} - G_{min}$

ΔG_{TH} = threshold ΔG dependent on material and test conditions

C,m,n,p = constant and exponents dependent on material and environment to be experimentally evaluated

G_c = critical G dependent on material and test conditions.

Equation (6) accounts for all of the observed effects on delamination growth rates, namely, no growth below

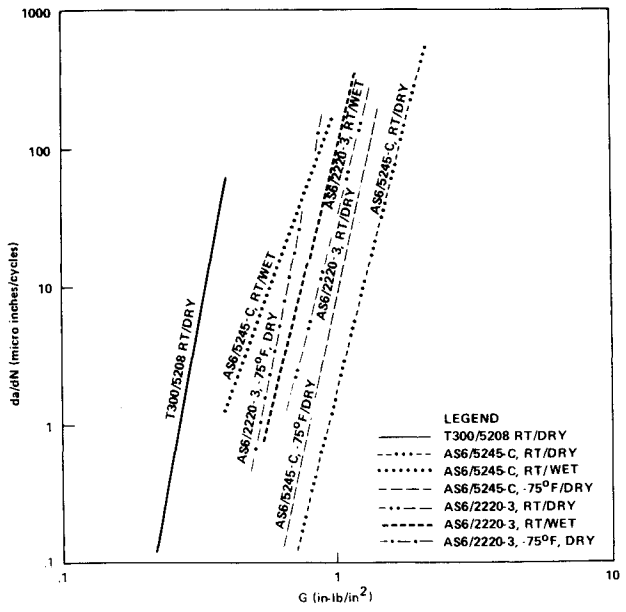

Fig. 7 Delamination growth rates for AS6/2220-3 and AS6/5245C.

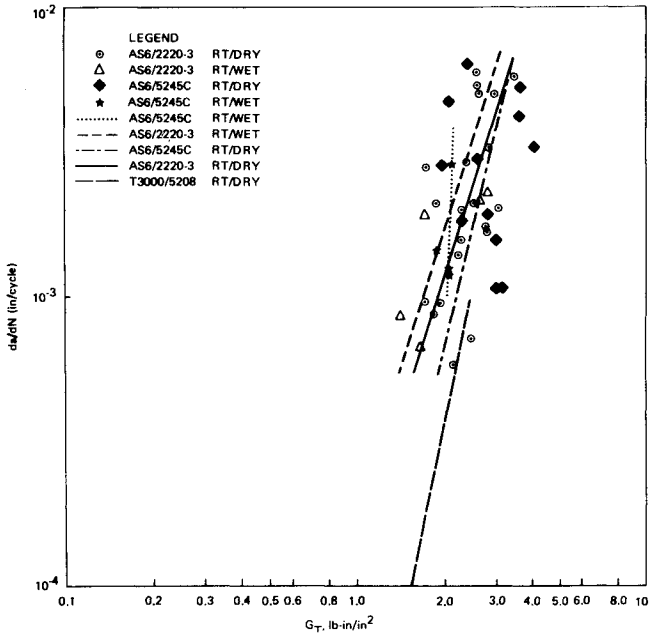

Fig. 8 Mixed mode delamination growth data for AS6/2220-3 and AS6/5245C materials.

threshold, stable linear da/dN vs G or ΔG behavior on a logarithmic plot, and extremely large da/dN values when the applied G approaches G_c. For most structural applications, except for the short fatigue life requirements for missiles and spacecraft, long fatigue life is required. Hence, rapid growth rates in region III are of little interest and the growth rate equation (6) can be simplified as follows:

$$\frac{da}{dN} = C(G_{max})^m (\Delta G - \Delta G_{TH})^n \tag{7}$$

Tests under the current program were conducted for only one R ratio ($R=0.05$) and a major portion of da/dN data comprised the stable region II well above the threshold. Equation (7) can be further simplified as

$$\frac{da}{dN} = C_1(G_{max})^n = C_2(\Delta G)^n \tag{8}$$

where n is redefined as $m+n$ of Eq. (7).

Table 8 Values of C_1 and n for delamination growth rates

Material	Environmental conditions	C_1	n
AS6/2220-3	RT/dry	2.66×10^{-5}	7.82
	RT/wet	9.05×10^{-5}	7.85
	−75°F/dry	3.97×10^{-4}	9.36
AS6/5245C	RT/dry	1.83×10^{-6}	7.65
	RT/wet	1.86×10^{-4}	5.35
	−75°F/dry	8.18×10^{-6}	8.97

The typical data shown in Fig. 6 was fitted with a least-square straight line with the above equation. The constant C_1 and the exponent n are given in Fig. 6 as well as in Table 8. Table 8 also gives values of C_1 and n for AS6/2220-3 and AS6/5245C for all of the environmental conditions tested. da/dN and G are in inch/cycle and pound-inch/inch squared, respectively.

Figure 7 shows a composite plot of da/dN vs G_{max} for AS6/2220-3 and AS6/5245C material systems at RT/dry, RT/wet, and −75°F/dry conditions. Figure 7 also includes da/dN for T300/5208 in RT/dry environment.[4] da/dN for T300/5208 for RT/dry is at least a factor of 10 faster than the fastest da/dN for AS6/2220-3 and AS6/5245C, which is for AS6/5245C in a RT/wet environment. For AS6/5245C, da/dN for RT/wet conditions is at least 100 times faster than RT/dry conditions. The results show the sensitivity of 5245C to wet environment. Figure 7 shows that da/dN for RT/wet and −75°F/dry conditions are approximately 3 and 10 times faster than the da/dN for RT/dry for AS6/2220-3. da/dN for AS6/5245C in a RT/wet environment is faster than AS6/2220-3 in −75°F/dry conditions also.

The exponent n for RT/dry mode I da/dN equation for $[0]_{24}$ DCB tests of T300/5208 is 8.02, which is about the same as for AS6/2220-3 and AS6/5245C materials.[4] An error of 21% in determination of G_{max} will introduce an error of 460% in da/dN. An error of 21% in G is not inconceivable and it is equivalent to a 10% error in the determination of the stress intensity factor in metallic materials. However, for the same error in the determination of G in the metals, error introduced in da/dN is less than 50%. The data for composites indicate that a much higher scatter factor will have to be used in the delamination growth life of the composites.

Constant amplitude fatigue tests on mixed mode I-II CLS specimens were conducted at $R=0.05$ and 5 Hz. Figure 8 shows a plot of mixed mode crack growth rates, da/dN vs the total strain energy release rate G_T for 10 specimens representing both material systems and RT/dry and RT/wet conditions. The peak G_T value in these cyclic tests was $0.90\ G_{Tc} \le G_T \le 0.95\ G_{Tc}$. Since the maximum G_T is close to G_{Tc}, significant variation in da/dN is observed. The maximum variation in da/dN at a given G_T is less than one order of magnitude, which is not uncommon for crack growth rates in composite materials. Another contributing factor to variations in G_T and da/dN was the delamination growth occurring out of its plane going from 0° into ±45° plies. All of these tests were conducted with 36.0 in. long specimens. Test specimen size could have also caused some problems. Tests were then conducted with 10.0 in. long specimens. Constant-amplitude fatigue tests on AS6/2220-3 CLS specimens (all 0° 10 ply thick 10.0 in. long by 0.50 in. wide) were conducted in RT/dry environment at 10 Hz. Cyclic tests were conducted at 50, 60, 70, 80, 90, and 95% of the critical load P_{cr}, as the maximum load and the minumum load was 2.5% of the critical load. Visual crack length observations were made at various number of cycles. The fracture surfaces of CLS specimens were examined with a scanning electron microscope (SEM) to see if any fatigue crack growth marks (striations) can be observed and correlated with the number of applied cycles and the visual cyclic crack growth rate. Striation markings were largely observed along the fiber/matrix interface with SEM. At times, striation mark-

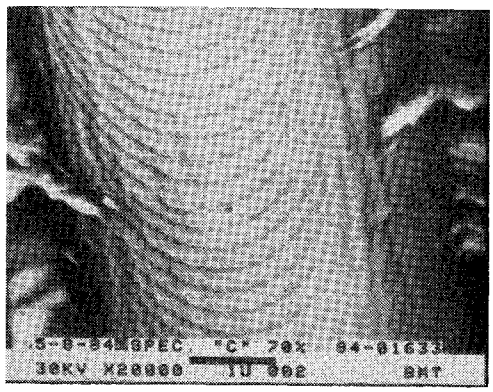

a) $P_{max} = 0.7\ P_{cr}$, $G_{Tmax} = 0.49\ G_{Tc}$.

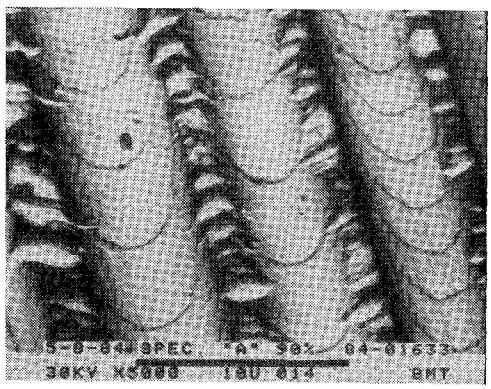

b) $P_{max} = 0.9\ P_{cr}$, $G_{Tmax} = 0.81\ G_{Tc}$.

Fig. 9 Electron fractograph of fracture surface of CLS specimen.

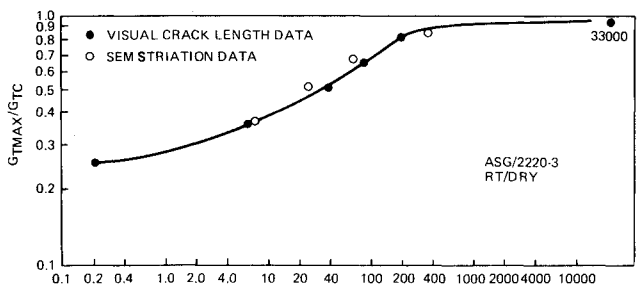

Fig. 10 Cyclic mode I-II delamination growth rates.

ings were also observed on the graphite fibers with the transmission electron microscope (TEM). Figure 9 shows electron fractographs indicating striation spacings and delamination growth rates generated for two maximum strain energy release rates, namely, 0.49 and 0.81 G_{Tc}. Delamination growth rates were obtained from striation spacings for various G_{Tmax}/G_{Tc} levels and were plotted against G_{Tmax}/G_{Tc} in Fig. 10. This figure also includes da/dN obtained from visual crack length observations. Correlation between da/dN from striation spacings and visual crack length data are excellent, as can be readily seen from Fig. 10. Striation markings and their correlations with visually or otherwise obtained da/dN data are common occurrences in metallic specimens under fatigue loadings. However, correlation with striation markings for graphite-epoxy composite material specimens has not been previously reported in the literature.

Figure 10 also shows three regions of delamination growth rates discussed previously. Threshold G_T is around 0.25 G_{Tc}. Region I (no or very slow) delamination growth occurs near $G_T \simeq 0.25\ G_{Tc}$. Region II growth occurs for $0.3\ G_{Tc} \leq G_T \leq 0.8\ G_{Tc}$. Region III (very rapid growth) occurs for $G_T > 0.8\ G_{Tc}$.

IV. Conclusions

1) AS6/2220-3 and AS6/5245C composite material systems are significantly tougher than currently used composite systems such as T300/5208.

2) G_{Ic} for AS6/5245C is at least 1.4 times greater than G_{Ic} for AS6/2220-3 in all of the environmental conditions tested.

3) $G_{IIc} \simeq 2.4\ G_{Ic}$ for AS6/2220-3 and $\simeq 1.5\ G_{Ic}$ for AS6/5245C material systems under RT/dry conditions.

4) Delamination growth rates da/dN for thermoset materials AS6/2220-3 and AS6/5245C can be well represented by the following equation for the tests conducted at one R value:

$$\frac{da}{dN} = C_1 G_{max}^n$$

5) da/dN for the RT/wet condition is at least 100 times faster than those for RT/dry conditions for AS6/5245C. For AS6/2220-3, -75°F/dry da/dN rates were fastest. da/dN for T300/5208 at even RT/dry conditions is at least 10 times faster than the fastest da/dN for AS6/5245C or AS6/2220-3 in any of the environments tested.

6) Striation markings were observed for mixed mode CLS specimens under fatigue loadings. The delamination growth rate can be computed directly from striation markings. da/dN vs G_{Tmax} from striations correlated very well with those from visually observed delamination length data.

Acknowledgments

The work reported here was performed at Boeing Military Airplane Company under IR&D funding. The authors wish to thank Messrs. J. A. Gertis and V. W. Rantala for test support.

References

[1]Wang, S. S., "Delamination Crack Growth in Unidirectional Fiber-Reinforced Composites Under Static and Cyclic Loading," *Composite Materials: Testing and Design*, ASTM STP674, 1979, pp. 642-663.

[2]Byers, B. A., "Behavior of Damaged Graphite/Epoxy Laminates under Compression Loading," NASA CR-159293, 1980.

[3]Wilkins, D. J., Eisenmann, J. R., Camin, R. A., Margolis, W. S., and Benson, R. A., "Characterizing Delamination Growth in Graphite-Epoxy," *Damage in Composite Materials*, ASTM STP775, 1982, pp. 168-183.

[4]Ramkumar, R. L., "Performance of a Quantitative Study of Instability-Related Delamination Growth," NASA CR 166046, 1983.

[5]Russell, A. J. and Street, K. N. "Moisture and Temperature Effects of the Mixed Mode Delamination Fracture of Unidirectional Graphite/Epoxy," Paper presented at ASTM Symposium on Delamination and Debonding of Materials, Pittsburgh, PA, Nov. 1983.

[6]Vonderkley, P. S., "Mode I-Mode II Delamination Fracture Toughness of a Undirectional Graphite/Epoxy System," Texas A&M University, College Station, Rept. MM 3724-81-15, 1981.

[7]Williams, J. G., O'Brien, T. K., and Chapman, A. J., "Comparison of Toughened Composite Laminates Using NASA Standard Damage Tolerance Tests," Paper presented at ACEE Composite Structures Technology Conference, NASA LaRC, Seattle, Aug. 1984.

[8]Ashizawa, M., "Improving Damage Tolerance of Laminated Composites through the Use of New Tough Resins," *Proceedings of Sixth Conference on Fibrous Composites in Structural Design*, Jan. 1983, pp. IV-21—IV-45.

[9]Whitney, J. M., Browning, C. E., and Hoogsteden, W., "A Double Cantilever Beam Test for Characterizing Mode I Delamination of Composite Materials," *Journal of Reinforced Plastics and Composites*, Vol. 1, 1982, pp. 297-313.

[10]O'Brien, T. K., "Interlaminar Fracture of Composites," NASA TM 85768, 1984.